

Weierstraß-Institut
für Angewandte Analysis und Stochastik
Leibniz-Institut im Forschungsverbund Berlin e. V.

Preprint

ISSN 2198-5855

**Three examples concerning the interaction of dry friction and
oscillations**

Alexander Mielke

submitted: June 2, 2017

Weierstrass Institute
Mohrenstr. 39
10117 Berlin
Germany
E-Mail: alexander.mielke@wias-berlin.de

Institut für Mathematik
Humboldt-Universität zu Berlin
Rudower Chaussee 25
12489 Berlin-Adlershof
Germany

No. 2405
Berlin 2017



2010 *Mathematics Subject Classification.* 34C55, 47J20, 49J40, 74N30.

Key words and phrases. Rate-independent friction, averaging of friction, play operator with time-dependent thresholds, locomotion, rate-and-state friction, Hopf bifurcation.

This research has been partially funded by Deutsche Forschungsgemeinschaft (DFG) through grant CRC 1114 "Scaling Cascades in Complex Systems", Project C05 "Effective models for interfaces with many scales".

Edited by
Weierstraß-Institut für Angewandte Analysis und Stochastik (WIAS)
Leibniz-Institut im Forschungsverbund Berlin e. V.
Mohrenstraße 39
10117 Berlin
Germany

Fax: +49 30 20372-303
E-Mail: preprint@wias-berlin.de
World Wide Web: <http://www.wias-berlin.de/>

Three examples concerning the interaction of dry friction and oscillations

Alexander Mielke

Abstract

We discuss recent work concerning the interaction of dry friction, which is a rate independent effect, and temporal oscillations. First, we consider the temporal averaging of highly oscillatory friction coefficients. Here the effective dry friction is obtained as an infimal convolution. Second, we show that simple models with state-dependent friction may induce a Hopf bifurcation, where constant shear rates give rise to periodic behavior where sticking phases alternate with sliding motion. The essential feature here is the dependence of the friction coefficient on the internal state, which has an internal relaxation time. Finally, we present a simple model for rocking toy animal where walking is made possible by a periodic motion of the body that unloads the legs to be moved.

1 Introduction

The phenomenon as well as the microscopic origins of dry friction are well studied (see e.g. [Pra28, Tom29, Pop10, PoG12, Mie12]). Here we understand dry friction in a generalized sense, namely in the sense of rate-independent friction that includes an activation threshold (critical force) to enable motion but then the friction force does not increase with the velocity (or more generally the rate). New nontrivial phenomena arise in cases where the critical force depends periodically on time, either given by an external process or because of the dependence on another state variable of the system. The three examples emphasize different realizations of this dependence.

We will study the effect that, in contrast to systems with viscous friction, systems with rate-independent friction tend to wait in a sticking mode until the relevant friction coefficient is small, and then they can make a very fast move (or even jump) to compensate for the past waiting time. To be more precise, we denote by (q, z) the state of a system, where z is the friction variable, and by \mathcal{R} the dissipation potential for the dry friction. Then $\mathcal{R}(q, z, \dot{q}, \dot{z})$ is nonnegative, convex in (\dot{q}, \dot{z}) and positively homogeneous of degree 1 in \dot{z} , namely $\mathcal{R}(q, z, \dot{q}, \gamma\dot{z}) = \gamma\mathcal{R}(q, z, \dot{q}, \dot{z})$ for all $\gamma > 0$. For simplicity we will assume that \mathcal{R} has an additive structure in the form

$$\mathcal{R}(q, z, \dot{q}, \dot{z}) = \mathcal{R}_{\text{vi}}(q, z, \dot{q}) + \mathcal{R}_{\text{RI}}(q, \dot{z}),$$

where “vi” stands for the viscous friction in the variable q , while “RI” stands for the rate-independent friction in the variable z . Note that we further simplified by assuming that \mathcal{R}_{RI} does not depend on z itself (see [BKS04, MiR07, MiR15] for more general cases).

The mathematical models we are interested in are given in the form

$$M\ddot{q} + \partial_{\dot{q}}\mathcal{R}_{\text{vi}}(q, z, \dot{q}) + D_q\mathcal{E}(t, q, z), \quad 0 \in \partial_{\dot{z}}\mathcal{R}_{\text{RI}}(q, \dot{z}) + D_z\mathcal{E}(t, q, z).$$

The simplest case of such a system occurs when $q(t)$ displays oscillatory behavior that is totally independent of the variable z , but \mathcal{R}_{RI} depends on q . In that case we may reduce to the equation for z alone and study

$$0 \in \mathcal{R}_{\text{RI}}(t/\varepsilon, \dot{z}) + D_z\mathcal{E}(t, z), \tag{1.1}$$

where $\varepsilon > 0$ is a small parameter indicating the ratio between the period of oscillations and the changes in the loading through $t \mapsto \mathcal{E}(t, z)$. A typical application is plate compactor (see Figure 1.1(A)), where an internal imbalance oscillates rapidly and thus changes the normal pressure in the contact friction. In Section 2 we summarize the results from [HeM17], where an explicit formula for the effective homogenized friction for $\varepsilon \rightarrow 0$ was derived, see Theorem 2.2 below.

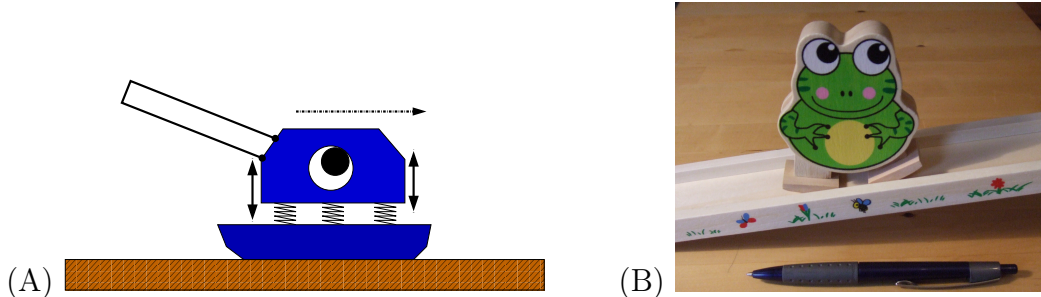


Figure 1.1: (A) Because of the in-built unbalance, the *plate compactor* vibrates vertically leading to an oscillatory normal pressure. When pushing the plate compactor horizontally it will move only when the normal pressure is very low. (B) The *toy ramp walker* in form of a frog walks down only, when alternating the weight between the rigid downhill leg and the hinged uphill leg.

In Section 3 we consider a system of the form

$$0 \in \partial_z \mathcal{R}_{\text{RI}}(\alpha, \dot{z}) + \nu \dot{z} + D_z \mathcal{E}(t, \alpha, z), \quad \dot{\alpha} = F(\alpha, z).$$

Our system is stimulated by applications in geophysics that relate to earthquakes and fault evolution, see [Rou14, PK*16, Pip17]. There so-called internal states α are needed to describe the relaxation effects after a sudden tectonic movement or change of shearing motions. We will show that a very simple system under constant shear loading can generate oscillatory behavior that is similar to the famous squeaking chalk on the blackboard or the vibrations arising when moving a rubber over a smooth surface.

Finally, Section 4 is devoted to the mechanism of walking of humans or animals. Clearly, an animal wants to reduce friction when moving the extremities on the ground. To do so, the weight on the leg to be moved has to be reduced. Thus, for making walking efficient it turns out that the body should oscillate in such a manner that without much extra energy the weight on the legs to be moved is minimal. Simple mechanical toys, where this interplay can easily be studied, are the so-called descending woodpecker (cf. [Pfe84]), the toy ramp walker, see Figure 1.1(B), and the rocking toy animal, see Figure 4.1. We refer to [GND14, DGN15, GiD16b, GiD16a] for models on locomotion for micro-machines or animals and to [RaN14] for the slip-stick dynamics of polymers on inhomogeneous surfaces.

We suggest a simple ODE model for the walking of simple mechanical toys such as the *rocking toy animal*, where the essential point is that there is some internal oscillatory mechanism that moves the normal pressure from one leg to the other such that the leg with lowest friction can move. One non-trivial feature is that the natural damping of the rocking motion has to be compensated by some energy supply, where the walking motion feeds energy back into the rocking motion.

2 Prescribed oscillatory friction

In this section we summarize the results from [HeM17] concerning the averaging of highly oscillatory rate-independent friction. As we will see there is a major difficulty intrinsic to

rate-independent systems that we only obtain a priori bounds for the rate in $BV([0, T]; X)$, but not in a weakly closed Banach space like $W^{1,p}([0, T]; X)$ for $p \in]1, \infty[$. Thus, even in the case of classical evolutionary variational inequalities we will not be able to pass to the limit variational inequality but have to use the more flexible formulation in terms of *energetic solutions*.

2.1 Evolutionary variational inequalities

While [HeM17] contains more general results, we restrict our discussion to the case of a Hilbert space Z and a quadratic energy $\mathcal{E}(t, z) = \frac{1}{2}\langle Az, z \rangle - \langle \ell(t), z \rangle$ with a loading $\ell \in W^{1,\infty}([0, T], Z^*)$ and a bounded, symmetric and positive definite linear operator $A : Z \rightarrow Z^*$. The dissipation potential is given in the form $\mathcal{R}_{\text{RI}}^\varepsilon(t, \dot{z}) = \Psi(t/\varepsilon, \dot{z})$, where $\Psi : \mathbb{S}^1 \times Z \rightarrow [0, \infty[$ is assumed to be continuous, and we assume $\Psi(0, v) \leq C\Psi(s, v) \leq C^2\Psi(0, v)$ for some $C > 1$ and all $(s, v) \in \mathbb{S} \times Z$.

Clearly, the equation $0 \in \partial_{\dot{z}}\Psi(t/\varepsilon, \dot{z}(t)) + Az(t) - \ell(t)$ is equivalent to the variational inequality

$$\forall_{\text{a.a.}} t \in [0, T] \quad \forall v \in Z : \quad \langle Az(t) - \ell(t), v - \dot{z}(t) \rangle + \Psi(t/\varepsilon, v) - \Psi(t/\varepsilon, \dot{z}(t)) \geq 0. \quad (2.1)$$

The key to the analysis in [HeM17] is that $z : [0, T] \rightarrow Z$ solves (2.1) if and only if it is an energetic solution, i.e.

$$\begin{aligned} \text{(S)} \quad & \forall t \in [0, T] \quad \forall \widehat{z} \in Z : \quad \mathcal{E}(t, z(t)) \leq \mathcal{E}(t, \widehat{z}) + \Psi(t/\varepsilon, \widehat{z} - z(t)); \\ \text{(E)} \quad & \mathcal{E}(T, z(T)) + \int_0^T \Psi(s/\varepsilon, \dot{z}(s)) \, ds \leq \mathcal{E}(0, z(0)) - \int_0^T \langle \dot{\ell}(s), z(s) \rangle \, ds. \end{aligned} \quad (2.2)$$

2.2 A scalar hysteresis operator

We now illustrate the difficulty in passing to the limit $\varepsilon \rightarrow 0$ in (2.1) by a very simple scalar hysteresis model by choosing $Z = \mathbb{R}$ and

$$\mathcal{E}(t, z) = \frac{1}{2}z^2 - \ell(t)z, \quad \Psi(s, \dot{z}) = \rho(s)|\dot{z}|, \quad \text{and} \quad z(0) = 0$$

with $\ell(t) = 5t - t^2$ and an arbitrary $\rho \in C^1(\mathbb{S})$ (where $\mathbb{S} := \mathbb{R}/\mathbb{Z}$) satisfying $\rho_{\min} := \min\{\rho(s) \mid s \in \mathbb{S}\} > 0$.

Starting from the initial condition $z(0) = 0$, we see that z cannot decrease but needs to lie in the stable interval $[\ell(t) - \rho(t/\varepsilon), \ell(t) + \rho(t/\varepsilon)]$, see (S) in (2.2). Thus, the solution $z_\varepsilon : [0, T] \rightarrow \mathbb{R}$ of $0 \in \rho(t/\varepsilon)\text{Sign}(\dot{z}(t)) + z(t) - \ell(t)$ has, for sufficiently small $\varepsilon > 0$, the representation

$$z_\varepsilon(t) = \begin{cases} \max\{0, \ell(\tau) - \rho(\tau/\varepsilon) \mid \tau \in [0, t]\} & \text{for } t \in [0, \frac{5}{2} + \sqrt{\rho_{\min}}], \\ \min\{\frac{25}{4} - \rho_{\min}, \ell(\tau) + \rho(\tau/\varepsilon) \mid \tau \in [\frac{5}{2} + \sqrt{\rho_{\min}}, t]\} & \text{for } t \geq \frac{5}{2} + \sqrt{\rho_{\min}}. \end{cases}$$

It can be checked by direct calculation that this is the unique solution. Moreover, we obtain uniform convergence to the limit solution given in the form

$$z_0(t) = \begin{cases} \max\{0, \ell(\tau) - \rho_{\min}\} & \text{for } t \in [0, \frac{5}{2} + \sqrt{\rho_{\min}}], \\ \min\{\frac{25}{4} - \rho_{\min}, \ell(\tau) + \rho_{\min}\} & \text{for } t \in [\frac{5}{2} + \sqrt{\rho_{\min}}, T]. \end{cases}$$

In particular, we have $\|z_\varepsilon - z_0\|_\infty \leq C\varepsilon$.

However, the situation for the rates $\dot{z}_\varepsilon : [0, T] \rightarrow \mathbb{R}$ is quite different. From the explicit formula we see that $\dot{z}_\varepsilon(t)$ either equals 0 (stiction) or $\dot{z}_\varepsilon(t) = \dot{\ell}(t) - \frac{1}{\varepsilon}\rho'(t/\varepsilon)$. Thus, within

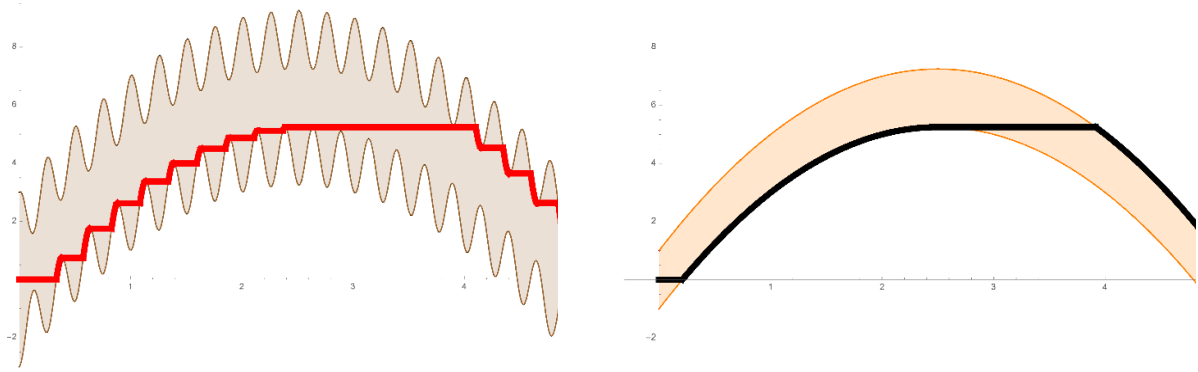


Figure 2.1: Left: the energetic solution $z_\varepsilon : [0, 5] \rightarrow \mathbb{R}$ for $\varepsilon = 0.1$. Right: the energetic solution $z_0 : [0, 5] \rightarrow \mathbb{R}$ for $\varepsilon = 0$. The limiting stable region (in orange) can be understood as the intersection of all stable regions for $\varepsilon > 0$.

the intervals $[k\varepsilon, (k+1)\varepsilon]$ we typically have $\dot{z}_\varepsilon = 0$ for most of the time and $\dot{z}_\varepsilon \approx 1/\varepsilon$ for intervals of length $O(\varepsilon^2)$, see Figure 2.1. As a consequence we conclude that \dot{z}_ε does not converge weakly to \dot{z}_0 in $L^p([0, T])$ for any $p \in [1, \infty[$. We only have $\dot{z}_\varepsilon \xrightarrow{*} \dot{z}_0$ in $M([0, T]) = C^0([0, T])^*$, i.e. in the sense of measures when testing with continuous test functions.

2.3 The averaging result for oscillatory friction

We now provide the announce averaging result, which can be understood in terms of an integral inf-convolutions as follows. We define

$$\Psi_{\text{av}}(V) := \inf \left\{ \int_{\mathbb{S}} \Psi(s, v(s)) \, ds \mid v \in L^1(\mathbb{S}), \int_{\mathbb{S}} v(s) \, ds = V \right\}. \quad (2.3)$$

This formulation justify the colloquial term that oscillatory rate-independent systems watch for the easiest opportunity to move: during the microscopic time $s = t/\varepsilon \in \mathbb{S}$ there is an instant such that moving in the direction $v(s) \in Z$ is optimal, hence the overall motion in direction $V \in Z$ will be decomposed into an oscillatory motion $s \mapsto v(s)$.

Example 2.1 For $Z = \mathbb{R}^2$ consider $\Psi(s, v) = (2 - \cos(2\pi s))|v_1| + (2 + \cos(2\pi s))|v_2|$. Then, $\Psi_{\text{av}}(v) = |v_1| + |v_2|$, since moving in z_1 -direction is optimal for $s \approx 0$ while motion in z_2 -direction is optimal for $s \approx 1/2$.

The first observation is that Ψ_{av} can be characterized in terms of the Legendre-Fenchel dual $\Psi^*(s, \xi) = \sup \{ \langle \xi, v \rangle - \Psi(s, v) \mid v \in Z \}$. From the 1-homogeneity of $\Psi(s, \cdot)$ we see that

$$\Psi^*(s, \cdot) = \chi_{K(s)}(\xi) = \begin{cases} 0 & \text{for } \xi \in K(s), \\ \infty & \text{otherwise,} \end{cases} \quad (2.4)$$

where $K(s) := \partial\Psi(s, 0)$ is a closed convex set containing $\xi = 0 \in Z^*$. In [HeM17, Prop. 3.6] it is shown that

$$\Psi_{\text{av}}^*(\xi) = \chi_{K_{\text{av}}}(\xi) \quad \text{with } K_{\text{av}} = \bigcap_{s \in \mathbb{S}} K(s).$$

The averaging result now reads as follows.

Theorem 2.2 (see [HeM17, Thm. 1.1]) *Consider a quadratic energetic system (Z, \mathcal{E}, Ψ) as in Section 2.1 and an initial condition $\widehat{z}_0 \in Z$ such that*

$$0 \in \partial_{\dot{z}}\Psi(s, 0) + A\widehat{z}_0 - \ell(0) \quad \text{for all } s \in \mathbb{S}.$$

Under the unique solutions $z_\varepsilon : [0, T] \rightarrow Z$ of (2.1) with $z_\varepsilon(0) = \widehat{z}_0$ satisfy $z_\varepsilon(t) \rightharpoonup z_0(t)$ in Z , where z_0 is the unique solution of the averaged equation

$$0 \in \partial\Psi_{\text{av}}(\dot{z}(t)) + Az(t) - \ell(t), \quad z_0(0) = \widehat{z}_0.$$

The proof relies heavily on the following asymptotic equicontinuity result:

$$\begin{aligned} \exists \text{ modulus of cont. } \omega \quad \forall \varepsilon \in]0, 1[\quad \forall t_1, t_2 \in [0, T] : \\ \|z_\varepsilon(t_2) - z_\varepsilon(t_1)\|_Z \leq \omega(\varepsilon) + \omega(|t_2 - t_1|). \end{aligned} \quad (2.5)$$

As is seen by the scalar example in Section 2.2 it is not possible to provide a better equicontinuity result. First it is then standard to extract a subsequence such that $z_{\varepsilon_n}(t)$ converges to some $z_0(t)$ weakly for all $t \in [0, T]$. The limit passage is then done in the energetic formulation (2.2). Using the definition of Ψ_{av} in (2.3) we have $\Psi_{\text{av}} \leq \Psi(s, \cdot)$, and it is easy to obtain the upper energy estimate (E), namely $\mathcal{E}(T, z_0(T)) + \int_0^T \Psi_{\text{av}}(\dot{z}_0) dt \leq \mathcal{E}(0, \widehat{z}_0) - \int_0^T \langle \dot{\ell}, z_0 \rangle ds$.

For the stability condition (S) we can use the equivalent formulation $0 \in \partial\Psi(t/\varepsilon, 0) + Az_\varepsilon(t) - \ell(t)$. Exploiting the equicontinuity (2.5) we can also have $z_\varepsilon(\widehat{\tau}(t, s, \varepsilon)) \rightharpoonup z_0(t)$ whenever $\widehat{\tau}(t, s, \varepsilon) \rightarrow 0$. Thus, we may choose $\widehat{\tau}(t, s, \varepsilon)$ such that $\widehat{\tau}(t, s, \varepsilon) \varepsilon \bmod 1 = s$ and obtain $0 \in \partial\Psi(s, 0) + Az_0(t) - \ell(t)$ for all $s \in \mathbb{S}$. By (2.4) we conclude $0 \in \partial\Psi_{\text{av}}(0) + Az_0(t) - \ell(t)$ which is (S) for the limit equation. By standard arguments we then conclude that z_0 is the desired unique solution.

3 Self-induced oscillations in state-dependent friction

The modeling of rate-and-state dependent friction is a classical area in geophysics as it describes basic mechanisms in the frictional movement of tectonic plates or faults in the earth crust, see [AbK13, PK*16] and [Rou14, PK*16] for more mathematical approaches. In [HMP17] the following work will be presented in the wider context of continuum mechanics. Here we rather restrict to a simple ODE in the spirit of the *spring-block sliders* studied in [AbK13].

Our simple scalar model of a block slider is described by the position $z(t)$ over the flat surface and a *state variable* α (that may be interpreted as a local temperature). The importance is that the friction coefficient μ for the rate-independent friction occurring through \dot{z} depends nontrivially on α , namely $\mu = \widetilde{\mu}(\alpha)$ with $\mu'(\alpha) < 0$, while friction $|\dot{z}|$ increases α .

For simplicity we restrict to the following simple coupled system:

$$0 \in \widetilde{\mu}(\alpha)\text{Sign}(\dot{z}(t)) + \nu\dot{z} + k(z(t) - \ell(t)), \quad \dot{\alpha} = \alpha_0 - \alpha + \widetilde{\mu}(\alpha)|\dot{z}| + \nu\dot{z}^2. \quad (3.1)$$

Here $k > 0$ is the elastic constant of the spring connecting the external loading $\ell(t)$ with the body, and $\nu \geq 0$ is a small viscosity coefficient in the friction law. Thus the friction is rate-dependent as well as state-dependent through α , namely for $\dot{z} > 0$ we have $\xi_{\text{frict}} = \widetilde{\mu}(\alpha) + \nu\dot{z}$. Note that the relaxation time for the state variable α was set to 1 without loss of generality.

For the later analysis it is advantageous to rewrite the first equation in (3.1) as an explicit ODE. Defining the functions

$$G(\xi, \alpha) := \begin{cases} (\xi - \tilde{\mu}(\alpha))/\nu & \text{for } \xi \geq \tilde{\mu}(\alpha), \\ 0 & \text{for } |\xi| \leq \tilde{\mu}(\alpha), \\ (\xi + \tilde{\mu}(\alpha))/\nu & \text{for } \xi \leq -\tilde{\mu}(\alpha), \end{cases}$$

we find the equivalent form

$$\dot{z} = G(k(\ell(t) - z), \alpha), \quad \dot{\alpha} = 1 - \alpha + k(\ell - z)G(k(\ell - z), \alpha). \quad (3.2)$$

The typical experiment is the model with a constant shear velocity V , i.e. $\ell(t) = Vt$. Indeed, the problem is translationally invariant if ℓ and z are changed together. Thus, it is useful to work with $V(t) = \dot{\ell}(t)$ and to consider the difference $U(t) = \ell(t) - z(t)$, which satisfies the ODE system

$$\dot{U}(t) = V(t) - G(kU(t), \alpha(t)), \quad \dot{\alpha}(t) = \alpha_0 - \alpha + kU(t)G(kU(t), \alpha(t)). \quad (3.3)$$

In [HMP17] the response of the system to varying shear rates $V(t)$ is studied in regimes where the system prefers to return into a steady state, whenever $V(t)$ has a plateau.

Here, we want to show that under suitable conditions on the function $\alpha \mapsto \mu(\alpha)$ the system displays self-induced oscillations for constant shear rates $V(t) \equiv V_*$. In that case (3.3) is a planar autonomous system which can be discussed in the phase plane for (U, α) . Without loss of generality we assume $V_* > 0$ and choose $k = \alpha_0 = 1$ for notational simplicity. We first calculate the equilibria (U_*, α_*) and note that no equilibria with $U_* \leq \tilde{\mu}(\alpha_*)$ can exist because then $G(U_*, \alpha_*) \leq 0$. Hence, the relations for equilibria reduce to

$$U_* = \tilde{\mu}(\alpha_*) + \nu V_* \quad \text{and} \quad \alpha_* = 1 + V_* U_*.$$

Using our major assumption $\tilde{\mu}'(\alpha) \leq 0$ we immediately see that there is a unique equilibrium determined by the relation $\alpha_* = 1 + V_* \tilde{\mu}(\alpha_*) + \nu V_*^2$. Clearly, α_* as a function of V_* is monotonously increasing from $\alpha_* = 1$ at $V_* = 0$.

To study the stability of the solution we calculate the linearization of the vector field $\frac{d}{dt} \begin{pmatrix} U \\ \alpha \end{pmatrix} = F(U, \alpha)$ in $q_* = (U_*, \alpha_*)$ giving the Jacobi matrix

$$DF(q_*) = \begin{pmatrix} -\partial_U G(q_*) & -\partial_\alpha G(q_*)/\nu \\ V_* + U_* \partial_U G(q_*) & -1 + U_* \partial_\alpha G(q_*) \end{pmatrix} = \begin{pmatrix} -1/\nu & -\tilde{\mu}'(\alpha_*) \\ V_* + U_*/\nu & -1 - U_* \tilde{\mu}'(\alpha_*)/\nu \end{pmatrix}.$$

As a result we find that the determinant $\det DF(q_*) = (1 - V_* \tilde{\mu}'(\alpha_*))/\nu$ is always positive. For the trace we obtain

$$\text{trace}(DF(q_*)) := -1 - (1 + U_* \tilde{\mu}'(\alpha_*))/\nu = -1 - \tilde{\mu}'(\alpha_*) V_* - (1 + \tilde{\mu}(\alpha_*) \tilde{\mu}'(\alpha_*))/\nu.$$

Clearly the equilibrium is stable if $\text{trace}(DF(q_*)) < 0$, undergoes a Hopf-bifurcation for $\text{trace}(DF(q_*)) = 0$, and is unstable for $\text{trace}(DF(q_*)) > 0$.

Theorem 3.1 (Periodic oscillations) *Assume that $V_* > 0$ is chosen such that the unique equilibrium $q_* = (U_*, \alpha_*)$ satisfies $\text{trace}(DF(q_*)) > 0$, then there exists a stable periodic orbit.*

Proof. The result follows from standard phase-plane arguments, since the equilibrium is unstable, and there exists a positively invariant region. Indeed, setting $U_{\max} = \tilde{\mu}(0) + \nu V_*$ we find $\dot{U} = V_* - G(U, \alpha) \leq 0$ for whenever $U \geq U_{\max}$. Hence, for $U \in [0, U_{\max}]$ we have $G(U, \alpha) \leq G_{\max} = U_{\max}^2/\nu$ and conclude that $\dot{\alpha} = 1 - \alpha + UG(U, \alpha) \leq 0$ for

$\alpha \geq \alpha_{\max} = 1 + G_{\max}$. Thus, the rectangle $[0, U_{\max}] \times [0, \alpha_{\max}]$ is positively invariant. By the Poincaré–Bendixson the existence of at least one limit cycle follows. Standard argument show that there must also be one stable periodic orbit. ■

We also want to understand the limit behavior $\nu \rightarrow 0$, which means that the friction part converges to its rate-independent limit while the variable α remains rate dependent. In that case, we expect that the oscillations become very fast with a period of order $O(\nu^\delta)$ for some $\delta > 0$. To analyze this case we consider a special scaling limit that shows a non-standard bifurcation. In particular, we assume that V is positive but also small with ν , i.e. we unfold ν and V simultaneously. Moreover, to simplify the notations we assume that the bifurcation takes place at $\alpha = 1$ already.

In particular, we consider the scalings

$$V = \nu \widehat{v}, \quad U = \widetilde{\mu}(\alpha) + \nu^2 \beta, \quad \alpha = 1 + \nu \gamma, \quad \widetilde{\mu}(\alpha) = \mu(\nu \gamma) - \sqrt{\nu} B,$$

where $B \in \mathbb{R}$ is an unfolding parameter, which is chosen with a particular scaling to generate periodic solutions with a phase of sticking and a phase of frictional sliding. The function μ is assumed to satisfy

$$1 + \mu(0)\mu'(0) = 0 \quad \text{with } \mu_0 := \mu(0) > 0 \text{ and } \mu'(0) = -1/\mu_0 < 0. \quad (3.4)$$

This gives the following equivalent system

$$\nu \dot{\beta} = \widehat{v} - \beta^+ - \mu'(\nu \gamma) \dot{\gamma}, \quad \dot{\gamma} = -\gamma + (\mu(\nu \gamma) - \sqrt{\nu} B + \nu^2 \beta) \beta^+,$$

where $\beta^+ := \max\{\beta, 0\}$. The special assumption in (3.4) leads to a cancellation when we insert the equation for $\dot{\gamma}$ into the equation for $\dot{\beta}$, namely

$$\begin{aligned} \dot{\beta} &= \frac{\widehat{v}}{\nu} + A(\nu, \gamma) \beta^+ + \frac{\mu'(\nu \gamma)}{\nu} \gamma - \nu \mu'(\nu \gamma) \beta \beta^+, \\ \dot{\gamma} &= -\gamma + (\mu(\nu \gamma) - \sqrt{\nu} B) \beta^+ + \nu^2 \beta \beta^+, \end{aligned} \quad (3.5)$$

where the coefficient $A(\nu, \gamma)$ stays is order $1/\sqrt{\nu}$ for $\nu \rightarrow 0$, namely

$$A(\nu, \gamma) := \frac{\mu'(\nu \gamma)(\sqrt{\nu} B - \mu(\nu \gamma)) - 1}{\nu} = \frac{B}{\mu_0 \sqrt{\nu}} + O(1)_{\nu \rightarrow 0},$$

where we used the first relation in (3.4).

The solutions we will construct below will satisfy estimates of the form $\gamma(t) \in [0, C]$ and $\beta(t) \leq [-C\widehat{v}/\nu, C/\sqrt{\nu}]$, hence it will be justified to drop the higher order terms. Using $b = B/\mu_0$ we will consider the simplified system

$$\dot{\beta} = \widehat{v} \nu (1 - b \sqrt{\nu}) + \frac{b}{\sqrt{\nu}} \beta^+ - \frac{1}{\nu \mu_0} \gamma, \quad \dot{\gamma} = \mu_0 \beta^+ - \gamma, \quad (3.6)$$

which is a piecewise linear system and has the unique steady state $(\beta_*, \gamma_*) = (\widehat{v}, \mu_0 \widehat{v})$. Since the system is positively homogeneous of degree 1, the solutions for general \widehat{v} are obtained from the solution $(\beta_1(t), \gamma_1(t))$ for $\widehat{v} = 1$ by a simple multiplication, namely $(\widehat{v} \beta_1(t), \widehat{v} \gamma_1(t))$.

We are especially interested in the case $b \in]0, 2[$ where the fixed point is an unstable focus with eigenvalues

$$\lambda_{1,2} = \frac{b/2}{\sqrt{\nu}} \pm i \frac{\omega_b}{\sqrt{\nu}} + O(1), \quad \text{where } \omega_b = \sqrt{1 - b^2/4}.$$

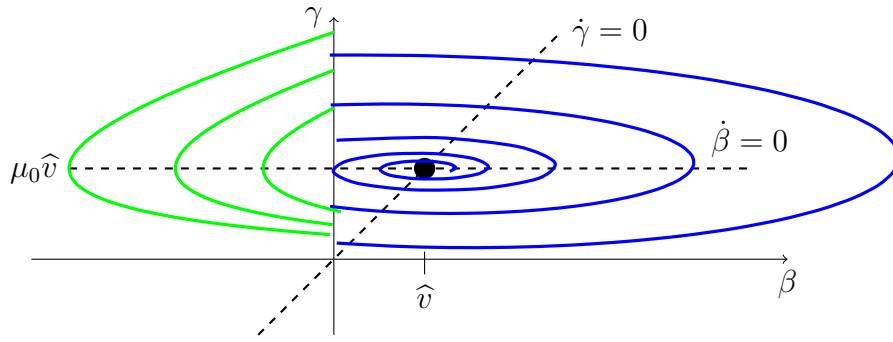


Figure 3.1: The phase plane for the piecewise linear system (3.6) for $\hat{v} = 1$ and $\mu_0 = 1$: For $\beta \geq 0$ we have an unstable focus, while for $\beta \leq 0$ we have the simple system $\dot{\beta} = 1/\nu - \gamma/(\nu\mu_0)$, $\dot{\gamma} = -\gamma$.

In the phase plane for (β, γ) we can construct periodic solutions by piecing together the piecewise linear systems, see Figure 3.1. For the explicit construction of a periodic orbits we decompose the axis $\{(0, \gamma) \mid \gamma \geq 0\}$ into the two parts $\{0\} \times A_j$ with

$$A_1 := [0, \mu_0 \hat{v}[\quad \text{and} \quad A_2 :=]\mu_0 \hat{v}, \infty[.$$

Then solutions starting in A_1 will move according to the unstable focus in $(\beta_*, \gamma_*) = (\hat{v}, \mu_0 \hat{v})$: First they rapidly move to the right, then turn slowly upwards, and reach $\dot{\beta} = 0$ when β is of order $1/\sqrt{\nu}$. Then, the solutions move rapidly back to the axis $\beta = 0$. Let us denote this Poincaré mapping by $\Phi^+ : A_1 \rightarrow A_2$. Since the motion between $\beta = 0$ and $\beta = \hat{v}$ only takes a time of order ν , it can be neglected compared to the travel time around the fixed point. Thus the travel time associated to Φ^+ is half the period, namely $\pi\omega_b/\sqrt{\nu}$. During that time the solutions are stretched, so that

$$\Phi^+(\nu, \cdot) : \begin{cases} A_1 & \rightarrow & A_2, \\ \gamma & \mapsto & \mu_0 \hat{v} + \rho_b(\mu_0 \hat{v} - \gamma) + O(\sqrt{\nu}), \end{cases}$$

with a stretching factor $\rho_b := e^{\pi b/(2\omega_b)} > 1$.

Similarly the linear flow for $\beta \leq 0$ provides a Poincaré map $\Phi^- : A_2 \rightarrow A_1$. As the solutions starting in A_2 are given by $\gamma(t) = e^{-(t-t_0)}\gamma(t_0)$ and $\nu\beta(t) = \hat{v}(t-t_0) + \frac{1}{\mu_0}(1-e^{t_0-t})\gamma(t_0)$ we obtain $\Phi^-(\gamma(t_0)) = \gamma(t_1)$, where $t_1 = t_0 + T$ is defined via $\hat{v}T = (1-e^{-T})\gamma(t_0)/\mu_0$. Since the function $\mathcal{B} :]0, \infty[\rightarrow]0, 1[$; $T \mapsto (1-e^{-T})/T$ is strictly decreasing it has a smooth inverse $\mathcal{C} :]0, 1[\rightarrow]1, \infty[$ which gives

$$\Phi^-(\nu, \cdot) : \begin{cases} A_2 & \rightarrow & A_1, \\ \gamma & \mapsto & e^{-\mathcal{C}(\mu_0 \hat{v}/\gamma)}\gamma, \end{cases}$$

which is even independent of ν , because this regime relates to the sticking phase $U < \mu(\alpha)$ where the viscosity ν is irrelevant. By construction it follows that Φ^- is convex and monotonously decreasing with slopes in $]-1, 0[$.

Periodic solutions are now obtained as fixed points of $\Psi := \Phi^- \circ \Phi^+ : A_1 \rightarrow A_1$. From the lowest order expansions of Φ^\pm we see that Ψ is convex and strictly increasing. Moreover $\Psi(\mu_0 \hat{v})$ is slightly below $\mu_0 \hat{v}$ and $\Psi'(\mu_0 \hat{v}) = \rho_b > 1$. Thus, there is a unique fixed point γ_b in the interior, while the fixed point at $\gamma = \mu_0 \hat{v}$ of the lowest-order expansion does not survive. As $\rho_b = e^{\pi b/(2\omega_b)}$ is strictly increasing with $b \in]0, 2[$ from 1 to ∞ , we see that $b \mapsto \gamma_b$ is strictly decreasing with limits $\gamma_0 = \mu_0 \hat{v}$ to $\gamma_2 = 0$. Since $0 < \Psi'(\gamma_b) < 1$, we also conclude that the associated periodic orbit is stable.

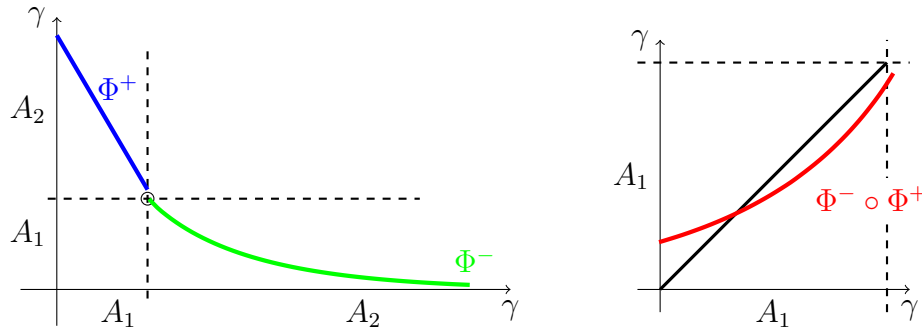


Figure 3.2: On the left, the two Poincaré maps $\Phi^+ : A_1 \rightarrow A_2$ and $\Phi^- : A_2 \rightarrow A_1$ are displayed. The right shows $\Phi^- \circ \Phi^+ : A_1 \rightarrow A_1$, where the unique fixed point gives to the stable limit cycle.

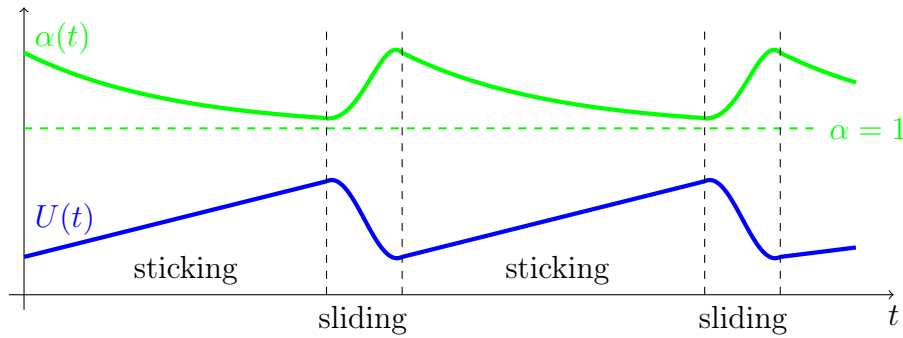


Figure 3.3: The periodic functions $U(t), \alpha(t)$ displaying long phases of sticking and short phases of fast slip.

The important observation is that the travel times in the two Poincaré mappings Φ^+ and Φ^- are quite different. The time with $\beta > 0$ is of order $\sqrt{\nu}\pi/\omega_b + O(\nu)$ while the time with $\beta < 0$ is of order 1. Thus, looking at the temporal behavior we have a relatively long period of sticking, while there is a relatively short period of sliding. Transforming our solutions back into the original variables we obtain, in the case $\beta > 0$ the expansion

$$U(t) = \mu(\nu\gamma) - \sqrt{\nu}B + \nu^2\beta = \mu_0 - \sqrt{\nu}B - \nu\frac{\gamma(t)}{\mu_0} + O(\nu^{3/2}), \quad \alpha(t) = 1 + \nu\gamma(t),$$

whereas in the case $\beta(t) < 0$ we have $\beta = O(1/\nu)$ and thus

$$U(t) = \mu_0 - \sqrt{\nu}B + \nu\hat{v}(t-t_k) - \nu\frac{\gamma(t_k)}{\mu_0} + O(\nu^{3/2}), \quad \alpha(t) = 1 + \nu e^{-(t-t_k)}\gamma(t_k),$$

where t_k is the last time, where the solution switched from $\beta > 0$ to $\beta < 0$. The behavior is illustrated in Figure 3.3.

We emphasize that all the solutions we have obtained in this scaling limit have a phase in the lower half plane, which means $U(t) \leq \tilde{\mu}(\alpha(t))$ and hence $\dot{U} = V$. In the original variables this means $\dot{z} = 0$ which is the sticking phase. Physically this means that the system rest for a short time until the shear has build up to reach the critical threshold. However, then the state α (e.g. the temperature) is increased so that the friction coefficient drops. Thus $z(t) = Vt - U(t)$ moves forward a lot and reduces the shear stress significantly. But then α again decreases and thus the friction coefficient again raises, which leads to the next sticking phase.

4 A model for the rocking toy animal

Our third example concerning the interaction of Coulomb friction and oscillations relates to a very simplistic model for walking of so-called *rocking toy animals*. A similar model could be derived for the toy ramp walker shown in Figure 1.1(B).

4.1 Description of the mechanical toy

The toy animal has two right and two left legs that usually move together so we identify them and speak of the right and the left leg. The toy is pulled forward by a string that hangs over the edge of a table, where a suitable weight provides a constant pulling force. A related walking toy is the ramp walker, which oscillates in the direction of walking. It has only two legs, the forward and the backward one, which are alternately loaded and unloaded, see Figure 4.1 for a pictures and two schematic views of a rocking toy cow.

This model has the following features:

- (i) Walking is a periodic motion that is enabled by perpendicular oscillations, which change the weight on the left and right legs.
- (ii) The force in the pulling string needs to be substantially less for the oscillating motion than for the sliding motion without oscillations. For very small pulling force no motion occurs.
- (iii) To compensate for damping in the perpendicular oscillations, energy has to be transferred from the forward motion into the perpendicular oscillation.

4.2 A model with inertia

We model the system of the toy animal by three degrees of freedom, i.e. we assume that both legs on the right side and both legs on the left side move together respectively and can be described by the average position $x_R(t) \in \mathbb{R}$ and $x_L(t) \in \mathbb{R}$. To simplify notations we abbreviate $\mathbf{x} = (x_R, x_L)$. The third degree of freedom is given by the angle ψ of the animals symmetry line against the vertical axis.

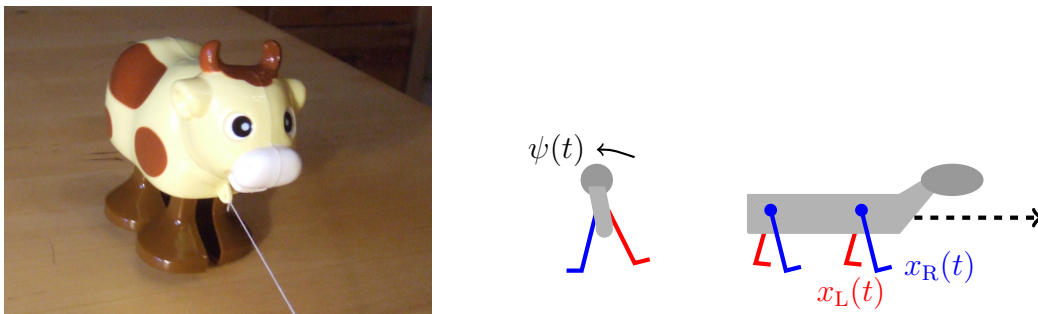


Figure 4.1: Rocking toy animal. Left: A weight beyond the table edge pulls the toy animal forward, while the perpendicular rocking motions allows the lifted legs to swing forward because of the reduced normal pressure. Middle: changes in the perpendicular rocking angle $\psi(t)$ lifts either the right or the left leg. Right: the string pulls the animal forward and increases the potential energy slightly when the hinge of a leg is moved over the leg's contact point.

The total energy $\mathcal{E}(\mathbf{x}, \psi, \dot{\mathbf{x}}, \dot{\psi}) = \mathcal{E}_{\text{ani}}(\mathbf{x}, \psi, \dot{\mathbf{x}}, \dot{\psi}) + \mathcal{E}_{\text{weight}}(\mathbf{x}, \dot{\mathbf{x}})$ is given by

$$\begin{aligned}\mathcal{E}_{\text{animal}}(\mathbf{x}, \psi, \dot{\mathbf{x}}, \dot{\psi}) &= \Phi(x_{\text{R}} - x_{\text{L}}, \psi) + \frac{m_{\text{b}}}{2}(\dot{x}_{\text{R}} + \dot{x}_{\text{L}})^2 + \frac{m_{\text{l}}}{2}((\dot{x}_{\text{R}})^2 + (\dot{x}_{\text{L}})^2) + \frac{I_{\text{b}}}{2}\dot{\psi}^2, \\ \mathcal{E}_{\text{weight}}(\mathbf{x}, \dot{\mathbf{x}}) &= -gm_{\text{W}}\frac{1}{2}(x_{\text{R}} + x_{\text{L}}) + \frac{m_{\text{W}}}{2}(\dot{x}_{\text{R}} + \dot{x}_{\text{L}})^2,\end{aligned}$$

where I_{b} is the rotational inertia of the body, and m_{b} , m_{l} , and m_{W} are the masses of the body, the legs, and the weight, respectively.

The main mechanism for walking originates from the dissipation, which we assume to have the form

$$\mathcal{R}(\mathbf{x}, \psi, \dot{\mathbf{x}}, \dot{\psi}) = \frac{\delta}{2}(\dot{\psi})^2 + (\rho + H_{\text{R}}(\psi))|\dot{x}_{\text{R}}| + (\rho + H_{\text{L}}(\psi))|\dot{x}_{\text{L}}| + \frac{\nu}{2}(\dot{x}_{\text{R}})^2 + \frac{\nu}{2}(\dot{x}_{\text{L}})^2,$$

where $\delta, \nu > 0$ induce simple viscous friction. The main feature of the model is the dependence of the rate-independent Coulomb friction of the two legs on the tilt angle ψ through the two functions H_{R} and H_{L} , which indicate the normal pressure times the friction coefficient on the right and the left leg, respectively, while $\rho > 0$ is the dry friction in the joints, which is independent of the normal pressure. We assume

$$\begin{aligned}H_{\text{R}}(\psi) + H_{\text{L}}(\psi) &= H_* = \text{const.}, \quad H_{\text{R}}(\psi) = H_{\text{L}}(-\psi), \\ H_{\text{R}}(\psi) = H_{\text{L}}(\psi) &= \frac{1}{2}H_* \text{ for } |\psi| \leq \psi_0, \quad H_{\text{R}}(\psi) = 0 \text{ for } \psi \geq \psi_1 > \psi_0.\end{aligned}$$

An important point in the modeling is that $0 < \rho \ll H_*/2$, i.e. the friction in the joints is much smaller than the friction of moving the non-rocking animal.

Denoting by $q = (\psi, x_{\text{R}}, x_{\text{L}})$ the state of the system, the equation to be studied is the damped Hamiltonian system

$$\frac{d}{dt} \left(\partial_{\dot{q}} \mathcal{E}(q, \dot{q}) \right) + \partial_{\dot{q}} \mathcal{R}(q, \dot{q}) + \partial_q \mathcal{E}(q, \dot{q}) = 0.$$

Thus, the full model takes the form of a coupled three-degrees of freedom system:

$$I_{\text{b}}\ddot{\psi} + \delta\dot{\psi} + \partial_{\psi}\Phi(x_{\text{R}} - x_{\text{L}}, \psi) = 0, \quad (4.1a)$$

$$\begin{aligned}(m_{\text{W}} + m_{\text{b}})(\ddot{x}_{\text{R}} + \ddot{x}_{\text{L}}) + m_{\text{l}}\ddot{x}_{\text{R}} \\ + \nu\dot{x}_{\text{R}} + (\rho + H_{\text{R}}(\psi))\text{Sign}(\dot{x}_{\text{R}}) + \partial_d\Phi(x_{\text{R}} - x_{\text{L}}, \psi) &= gm_{\text{W}}/2,\end{aligned} \quad (4.1b)$$

$$\begin{aligned}(m_{\text{W}} + m_{\text{b}})(\ddot{x}_{\text{R}} + \ddot{x}_{\text{L}}) + m_{\text{l}}\ddot{x}_{\text{L}} \\ + \nu\dot{x}_{\text{L}} + (\rho + H_{\text{L}}(\psi))\text{Sign}(\dot{x}_{\text{L}}) - \partial_d\Phi(x_{\text{R}} - x_{\text{L}}, \psi) &= gm_{\text{W}}/2,\end{aligned} \quad (4.1c)$$

where $d = x_{\text{R}} - x_{\text{L}}$ is the (signed) distance between the right and the left leg.

The main mathematical task in studying this model is to show that there are time-periodic translating motions, i.e.

$$\psi(t) = \Psi_{\text{per}}(t), \quad x_{\text{R}}(t) = vt + R_{\text{per}}(t), \quad y_{\text{L}}(t) = vt + L_{\text{per}}(t),$$

where v is the average walking speed while $(\Psi_{\text{per}}, R_{\text{per}}, L_{\text{per}}) : \mathbb{R} \rightarrow \mathbb{R}^3$ is periodic. The trivial solution is the non-rocking solution $(\Psi_{\text{per}}, R_{\text{per}}, L_{\text{per}}) \equiv 0$, where the velocity and the pulling force are related by

$$\nu v + \rho + \frac{1}{2}H_* = \frac{1}{2}gm_{\text{W}}.$$

Thus, even for arbitrary small velocities $v > 0$, the pulling force must overcome the full Coulomb friction for the full weight of the toy. The point is that a symmetry breaking

leading to an oscillatory behavior can lead to larger velocities v even for much lower pulling forces gm_W .

In principle, this model could be studied for the desired oscillatory behavior, but we will simplify the model further such that the existence of relevant periodic motions can be shown more easily.

4.3 A simplified model without translational inertia

We consider a simplified model, where we neglect inertial effects in the translation direction but not in the transverse oscillations. Thus, we neglect all terms in the energy arising through (\dot{x}_R, \dot{x}_L) . Similarly, we may keep the

$$\text{pulling force } P := gm_W$$

constant and then set $m_l = m_b = m_W = 0$. Moreover, we choose a simple quadratic energy potential, where it is important to couple the leg distance $d = x_R - x_L$ and the angle ψ , namely

$$\Phi(d, \psi) = \frac{a}{2}d^2 + \frac{b}{2}\psi^2 - cd\psi \quad \text{with } a, b, ab - c^2 > 0.$$

Hence, the trivial symmetric state $(x_R - x_L, \psi) = (0, 0)$ is stable. It is important to have $c > 0$, which reflects the fact of symmetry breaking for the walking toy: the tilt angle restoring force is $\partial_\psi \Phi(d, \psi) = b\psi - cd$, so if $d > 0$ (right leg before left one) then there is a stronger tendency to fall to the left than to fall to the right.

The simplified system now takes the form

$$I_b \ddot{\psi} + \delta \dot{\psi} + b\psi - c(x_R - x_L) = 0, \quad (4.2a)$$

$$(\rho + H_R(\psi)) \text{Sign}(\dot{x}_R) + a(x_R - x_L) - c\psi = P, \quad (4.2b)$$

$$(\rho + H_L(\psi)) \text{Sign}(\dot{x}_L) - a(x_R - x_L) + c\psi = P. \quad (4.2c)$$

The equations (4.2b) and (4.2c) for x_R and x_L , respectively, are simple play operators (cf. [Vis94, BrS96]), however the thresholds $\rho + H_{R,L}(\psi(t))$ vary in time and are even influenced by \mathbf{x} through (4.2a).

Nevertheless, we will be able to reduce this coupled system to an oscillator for ψ involving a hysteresis operator induced by the relations for x_R and x_L . For this we first observe that the relations (4.2b) and (4.2c) restrict the leg distance $d(t) := x_R(t) - x_L(t)$ because of $\text{Sign}(\dot{x}_{R,L}) \in [-1, 1]$ as follows:

$$g(t) \in [G_R^-(\psi), G_R^+(\psi)] \cap [G_L^-(\psi), G_L^+(\psi)] \quad \text{with}$$

$$G_R^\pm(\psi) = \frac{1}{a} \left(P + c\psi \pm (\rho + H_R(\psi)) \right),$$

$$G_L^\pm(\psi) = \frac{1}{a} \left(-P + c\psi \pm (\rho + H_L(\psi)) \right).$$

We now explain that for a given continuous function $t \mapsto \psi(t)$ there is a hysteresis operator \mathcal{H} such that the output $d(t) = \mathcal{H}[\psi(\cdot)](t)$ is explicitly given through the boundary curves $G^+ > G^-$ via the formulas

$$G^+(\psi) := \min\{G_L^+(\psi), G_R^+(\psi)\} \quad \text{and} \quad G^-(\psi) := \max\{G_L^-(\psi), G_R^-(\psi)\}.$$

Of most interest are the local minimum of G^+ at $\psi_1 > 0$ and the local maximum of G^- at $-\psi_1 < 0$ (see $\psi_1 = 1$ in Figure 4.2). For simplicity, we choose constants $\psi_*, H_* > 0$

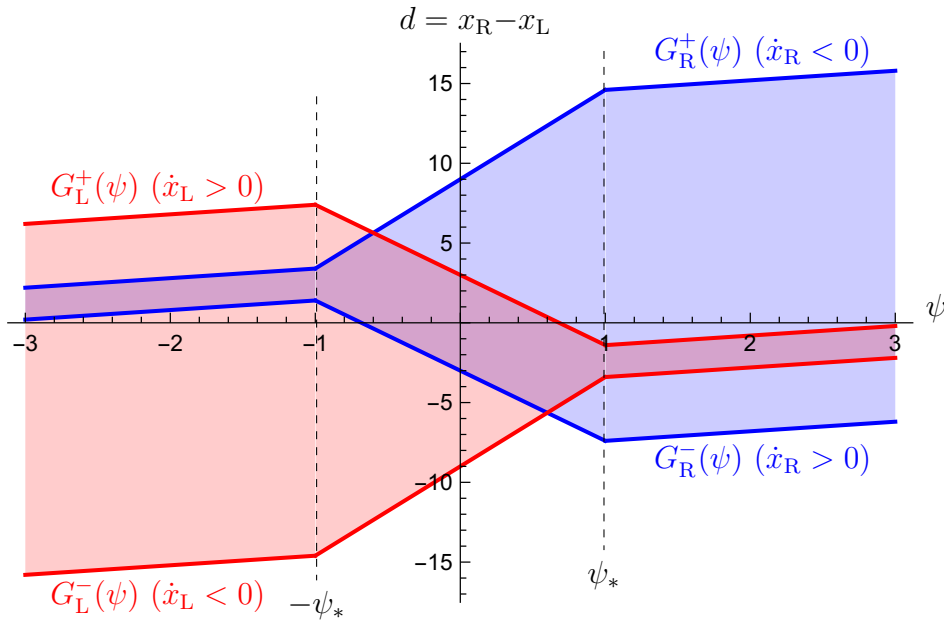


Figure 4.2: Sketch of the sets $[G_R^-(\psi), G_R^+(\psi)]$ and $[G_L^-(\psi), G_L^+(\psi)]$. The solutions have to stay inside the intersection of the two shaded regions. We have $\dot{d} \leq 0$ at the upper curve $G^+ : \psi \mapsto \min\{G_L^+(\psi), G_R^+(\psi)\}$ and $\dot{d} \geq 0$ at the lower curve $G^- : \psi \mapsto \max\{G_L^-(\psi), G_R^-(\psi)\}$. Between these two curves we have $\dot{d} \equiv 0$.

with $H_* > 2c\psi_*$ and restrict to the piecewise affine case

$$H_R(\psi) = \begin{cases} 0 & \text{for } \psi \leq -\psi_*, \\ H_*(\psi + \psi_*)/(2\psi_*) & \text{for } |\psi| \leq \psi_*, \\ H_* & \text{for } \psi \geq \psi_*. \end{cases}$$

Thus, we can calculate the local minimum of G^+ and the local maximum of G^- explicitly, namely

$$(\psi_*, -\mathbf{X}) \text{ and } (-\psi_*, \mathbf{X}) \quad \text{with } \mathbf{X} := \frac{1}{a}(P - \rho - c\psi_*),$$

where we further assume $\mathbf{X} > 0$ (i.e. $P > \rho + c\psi_*$) and $H_* > 2P$.

4.4 Restriction to simple period motions

We now restrict to a special period motion where the hysteresis operator can be replaced by an ordinary function, namely in the region

$$\psi \in [-\psi_2, \psi_2] \text{ with } \psi_2 := 2\rho/c + \psi_*.$$

where we set $d(t) = \mathbf{G}(\psi(t), \dot{\psi}(t))$ with

$$\mathbf{G}(\psi, \dot{\psi}) = \begin{cases} \Gamma(\psi) & \text{if } \dot{\psi} \geq 0, \\ -\Gamma(-\psi) & \text{if } \dot{\psi} < 0. \end{cases} \quad \text{with } \Gamma(\psi) := \begin{cases} \mathbf{X} & \text{for } \psi \in [-\psi_2, \psi_3], \\ G_L^+(\psi) & \text{for } [\psi_3, \psi_*], \\ -\mathbf{X} & \text{for } \psi \in [\psi_*, \psi_2], \end{cases}$$

where ψ_3 is the unique solution of $\mathbf{X} = G_L^+(\psi)$ in $[0, \psi_*]$. (Note that $G_L^+(0) = (\rho + H_*/2 - D)/a > 0$ and $G_L^+(\psi_*) = -\mathbf{X} < 0$.)

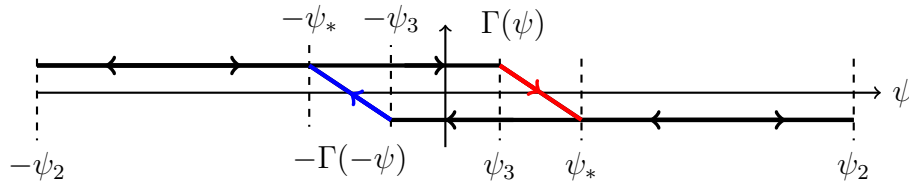


Figure 4.3: The two branches of the function $\mathbf{G}(\psi, \dot{\psi})$, namely $\Gamma(\psi)$ for $\dot{\psi} > 0$ and $-\Gamma(-\psi)$ for $\dot{\psi} < 0$.

Thus, we have eliminated all dependence on the variables x_R and x_L and are left with a nonlinear oscillator equation for ψ , namely

$$I_b \ddot{\psi} + \delta \dot{\psi} + b\psi - c\mathbf{G}(\psi, \dot{\psi}) = 0.$$

Note that this is a piecewise linear equation, where \mathbf{G} switches between the two constant values $\pm \mathbf{X}$ with some linear transition region inbetween. The point is that this switching feeds energy into the system which may compensate the damping through $\delta > 0$.

It is now possible to show that there are suitable parameters such that this equation has a periodic orbit. This can be done in a similar way using Poincaré sections as in the previous section. We refer to subsequent work for precise statements and proofs. We conclude with some numerical results showing the convergence into a stable periodic orbit for ψ and $\mathbf{x}(t) - v(t, t)$ with a suitable walking speed $v > 0$.

Acknowledgements. The authors is grateful to Martin Heida and Elais Pipping for stimulating discussions. The research was partially supported by DFG via the project C05 *Effective Models for Interfaces with Many Scales* within the SFB 1114 *Scaling Cascades in Complex Systems*.

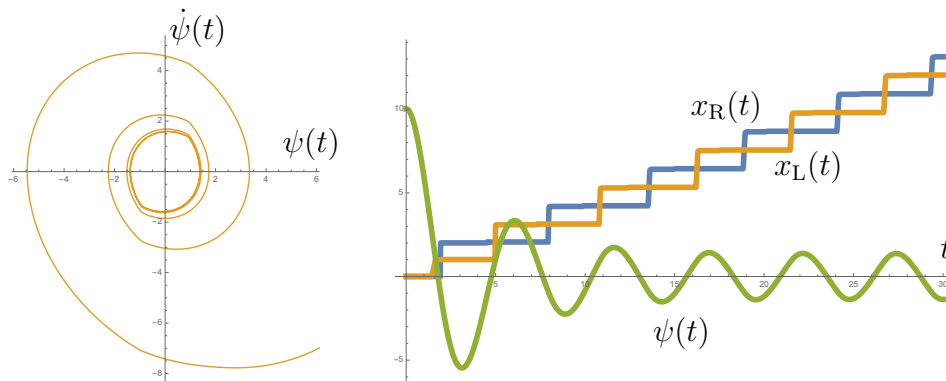


Figure 4.4: Simulation for the simplified system (4.2). Left: $(\psi(t), \dot{\psi}(t))$ spirals towards a stable limit cycle. Right: The functions $\psi(t)$, $x_R(t)$, and $x_L(t)$ show periodic behavior up to a linear translational mode for $x_{R,L}$.

References

- [AbK13] Y. ABE and N. KATO. Complex earthquake cycle simulations using a two-degree-of-freedom spring-block model with a rate- and state-friction law. *Pure Appl. Geophysics*, 170(5), 745–765, 2013.
- [BKS04] M. BROKATE, P. KREJČÍ, and H. SCHNABEL. On uniqueness in evolution quasivariational inequalities. *J. Convex Anal.*, 11, 111–130, 2004.
- [BrS96] M. BROKATE and J. SPREKELS. *Hysteresis and Phase Transitions*. Springer-Verlag, New York, 1996.
- [DGN15] A. DESIMONE, P. GIDONI, and G. NOSELLI. Liquid crystal elastomer strips as soft crawlers. *J. Mech. Physics Solids*, 84, 254–272, 2015.
- [GiD16a] P. GIDONI and A. DESIMONE. On the genesis of directional friction through bristle-like mediating elements crawler. *arXiv:1602.05611*, 2016.
- [GiD16b] P. GIDONI and A. DESIMONE. Stasis domains and slip surfaces in the locomotion of a bio-inspired two-segment crawler. *Meccanica*, 2016. In press.
- [GND14] P. GIDONI, G. NOSELLI, and A. DESIMONE. Crawling on directional surfaces. *Int. J. Non-Linear Mech.*, 61, 65–73, 2014.
- [HeM17] M. HEIDA and A. MIELKE. Averaging of time-periodic dissipation potentials in rate-independent processes. *Discr. Cont. Dynam. Systems Ser. S*, 2017. To appear. WIAS preprint 2336.
- [HMP17] M. HEIDA, A. MIELKE, and E. PIPPING. Rate-and-state friction from a thermodynamical viewpoint. *In preparation*, 2017.
- [Mie12] A. MIELKE. Emergence of rate-independent dissipation from viscous systems with wiggly energies. *Contin. Mech. Thermodyn.*, 24(4), 591–606, 2012.
- [MiR07] A. MIELKE and R. ROSSI. Existence and uniqueness results for a class of rate-independent hysteresis problems. *Math. Models Meth. Appl. Sci. (M³AS)*, 17(1), 81–123, 2007.
- [MiR15] A. MIELKE and T. ROUBÍČEK. *Rate-Independent Systems: Theory and Application*. Applied Mathematical Sciences, Vol. 193. Springer New York, 2015.
- [Pfe84] F. PFEIFFER. Mechanische Systeme mit un stetigen Übergängen. *Ingenieur-Archiv*, 54, 232–240, 1984. (In German).
- [Pip17] E. PIPPING. Existence of long-time solutions to dynamic problems of viscoelasticity with rate-and-state friction. *arXiv:1703.04289v1*, 2017.
- [PK*16] E. PIPPING, R. KORNHUBER, M. ROSENAU, and O. ONCKEN. On the efficient and reliable numerical solution of rate-and-state friction problems. *Geophys. J. Int.*, 204(3), 1858–1866, 2016.
- [PoG12] V. L. POPOV and J. A. T. GRAY. Prandtl-Tomlinson model: History and applications in friction, plasticity, and nanotechnologies. *Z. angew. Math. Mech. (ZAMM)*, 92(9), 692–708, 2012.
- [Pop10] V. L. POPOV. *Contact Mechanics and Friction*. Springer, 2010.
- [Pra28] L. PRANDTL. Gedankenmodell zur kinetischen Theorie der festen Körper. *Z. angew. Math. Mech. (ZAMM)*, 8, 85–106, 1928.

- [RaN14] M. RADTKE and R. R. NETZ. Shear-induced dynamics of polymeric globules at adsorbing homogeneous and inhomogeneous surfaces. *Europ. Phys. J. E*, 37(20), 11, 2014.
- [Rou14] T. ROUBÍČEK. A note about the rate-and-state-dependent friction model in a thermodynamical framework of the biot-type equation. *Geophys. J. Int.*, 199(1), 286–295, 2014.
- [Tom29] G. A. TOMLINSON. A molecular theory of friction. *Philos. Mag.*, 7, 905–939, 1929.
- [Vis94] A. VISINTIN. *Differential Models of Hysteresis*. Springer-Verlag, Berlin, 1994.